THE ASTROPHYSICAL JOURNAL, 347:490–495, 1989 December 1


# ORBITAL MIGRATION OF PROTOPLANETS: THE INERTIAL LIMIT

WILLIAM R. WARD[1]
Jet Propulsion Laboratory, California Institute of Technology
AND
KERRY HOURIGAN
Division of Building, Construction and Engineering, CSIRO
*Received 1988 December 26; accepted 1989 June 8*

## ABSTRACT

The dynamical evolution of a disk and the orbital migration of an embedded protoplanet are examined. We show how the migration of a protoplanet due to density waves torques can suppress the tendency for tidal truncation of the disk. A critical mass is determined as a function of the disk properties that represents the limiting mass that can sustain drift without stalling. This inertial limit is derived analytically, using a quasi-steady state theory, and confirmed by numerical experiment. This result contradicts the claim of Lin and Papaloizou that such a limit does not exist. Orbital mobility of objects due to density wave torques may have played an important role in the early evolution of the solar system.

*Subject headings:* hydrodynamics — planets: formation — solar system: general

## I. INTRODUCTION

We reexamine the mass limit proposed by Hourigan and Ward (1984; hereafter Paper I) for the orbital drift of a planetesimal driven by density wave interaction with the solar nebula. Drift can be caused by differential Lindblad torques arising from asymmetries in the nebula's rotation and structure. Stalling occurs when the planetesimal opens a gap in the disk. Since torques are proportional to the square of the perturber mass, $m$, the time scale for opening a gap is $\tau_{\rm gap} \propto m^{-2}$, while the characteristic drift time is $\tau_{\rm drift} \propto m^{-1}$. This suggests that there is a limiting mass, $m_i$, below which a planetesimal drifts too quickly to allow gap formation. This "inertial" limit was first calculated by Hourigan and Ward by employing an impulse approximation of the density wave torque devised by Lin and Papaloizou (1979).

This problem has subsequently been studied numerically by Lin and Papaloizou (1986; hereafter LP86) using essentially the same impulse model. They concluded that our proposed limit did not exist, but their paper contains several misinterpretations of our model. We demonstrate here that their work largely reproduces ours, and that their case studies are consistent with our predictions.

## II. INERTIAL LIMIT

### a) *Equations of Motion*

We start by reviewing the original derivation of the inertial limit. Consider a planetesimal embedded in a Keplerian sheet. The tidal effects on nearby portions of the disk result in a mutual torque that can be approximated by integrating over a torque density of the form.

$$\frac{dT}{dr} \sim \text{sgn}\,(r - r_p)\,\frac{9}{4} f\,\frac{G^2 m^2 \sigma}{r(\Omega - \Omega_p)^2 (r - r_p)^2}\,, \tag{1}$$

where $f$ is a constant of order unity. The drift rate of the planetesimal is found by equating the rate of change of its angular momentum, $d(mr_p^2\,\Omega_p)/dt$, to the total disk-integrated torque. The implied radial velocity $v_p \equiv dr_p/dt$, of the planetesimal is

$$v_p = \frac{2}{m r_p \Omega_p} \int -\left(\frac{dT}{dr}\right) dr\,. \tag{2}$$

The evolution of the disk due to the reaction torque is described by Euler's equation,

$$\frac{D}{Dt}\,(\delta m l) = \pi \sigma r^2 \Omega v\,\delta r = \frac{dT}{dr}\,\delta r\,, \tag{3}$$

where $\delta m = 2\pi\sigma r\,\delta r$ is an annulus of the disk, $l = r^2\Omega = \sqrt{GM_\odot r}$ is the specific angular momentum for Keplerian rotation, and $v$ represents the radial velocity of disk material (e.g., Lynden-Bell and Pringle 1974). The differential angular velocity in equation (1) is replaced by $\Omega - \Omega_p \sim (r - r_p)d\Omega/dr \sim -(3/2)\Omega(r - r_p)/r$ to lowest order accuracy. We treat $r - r_p \equiv x$ and $\sigma(x)$ as the only rapidly varying quantities and ignore changes in slow variables. When not differenced, we set $r = r_p$ and $\Omega = \Omega_p$. The planetesimal mass is normalized to that of the primary $\mu = m/M_\odot$. The planetesimal and fluid velocities become

$$v_p \sim -2 f \mu r^5 \frac{r\Omega}{M_\odot} \int_{-\infty}^{\infty} \text{sgn}\,(x)\,\frac{\sigma(x)}{x^4}\,dx\,, \tag{4}$$

$$v \sim \text{sgn}\,(x)\,\frac{f}{\pi}\,\mu^2 r\Omega \left(\frac{r}{x}\right)^4\,, \tag{5}$$

where the integration limits have been extended to $\pm\infty$ with little error. The divergent behavior of equations (4) and (5) as $|x| \to 0$ is not real. The tidal torque originates from strong interaction with the disk at Lindblad resonances (e.g., Goldreich and Tremaine 1979). Resonances lying closer than a scale height $h \sim c/\Omega$ ($c$ being the gas sound speed) to the protoplanet have perturbation wavelengths shorter than $h$ and a suppressed response (i.e., the torque cutoff zone; Goldreich and Tremain 1980). We introduce an ad hoc cutoff function $f(x)$ into $dT/dr$ that equals unity for $|x| \geq h$, but rapidly approaches zero for $|x| < h$.

[1] Also Department of Physics, Harvey Mudd College, Claremont, CA 91711

*b) Tidal Response of the Disk*

The migrating planetesimal should create a disturbance in the disk that tracks the planet. In a co-moving coordinate system centered on the planetesimal, the fluid velocity is $v' = v - v_p$ and produces a radial flux $F = 2\pi r\sigma v'$. The equation of continuity in the moving frame is

$$\frac{\partial\sigma}{\partial t} = -\frac{1}{2\pi r}\frac{\partial F}{\partial x} \approx -\frac{\partial}{\partial x}(\sigma v') \,. \tag{6}$$

We seek a quasi-steady state for which $\partial\sigma/\partial t \approx 0$. This implies $F \approx$ constant. This constant can be evaluated upstream from the perturber, out of range of its influence ($v \to 0$) where $F \to -2\pi r\sigma_0 v_p$, $\sigma_0$ being the unperturbed surface density. If $\sigma_0 =$ constant, $\partial\sigma/\partial t = 0$ and the flux is unchanged from its unperturbed value. The perturbed density is found from

$$F = 2\pi r\sigma v' = 2\pi r\sigma(v - v_p) = -2\pi r\sigma_0 v_p \,. \tag{7}$$

This is an inviscid form of equation (13) given in Paper I. With the aid of equation (5) we find

$$\sigma = \frac{v_p\sigma_0}{v_p - v} = \sigma_0\left[1 - f(x)\frac{\mathrm{sgn}\,(x)}{H^4}\left(\frac{h}{x}\right)^4\right]^{-1} , \tag{8}$$

where the dimensionless parameter, $H$, is defined by the combination

$$\frac{1}{H^4} = \frac{f\mu^2}{\pi}\left(\frac{r\Omega}{v_p}\right)\left(\frac{r}{h}\right)^4 \equiv \Lambda \,. \tag{9}$$

Equation (8) describes the disk response to the protoplanet induced tides and is in the form of a traveling wave, $\sigma(r - v_p t)$, moving with the perturber. The disturbance becomes more pronounced with increasing mass, $\mu$, but less pronounced with increasing drift speed, $v_p$. Hence, $\Lambda$ is a measure of disturbance strength. Lin and Papaloizou incorrectly interpreted equation (8) as representing a "fixed," "arbitrarily imposed" density profile. In fact, its calculation is the key ingredient to determining the mass limit.

For convenience, our computations in Paper I employed a cutoff function $[f(x) = (x/h)^4]$, which produced a constant magnitude torque inside the cut-off zone with a sign reversal at $x = 0$. Lin and Papaloizou (LP86) chose an effective form $f(x) = |x/h|^5$ so that the torque varied linearly with $x$ inside the zone. Neither form matches the true cutoff function computed numerically by Goldreich and Tremaine (1980), but these differences are of minor importance to our purposes here.

Substitution of equation (8) into equation (4) allows us to calculate the *feedback* contribution to the planetesimal drift rate

$$\Delta v_p \sim -2f\mu\frac{\sigma_0 r^2}{M_\odot}\left(\frac{r}{h}\right)^3 (r\Omega)H^3 G_1(H) \,, \tag{10}$$

where for the "constant" torque cutoff of Paper I,[2]

$$G_1(H) = \frac{2H}{H^8 - 1} + \frac{1}{4}\ln\left(\frac{H+1}{H-1}\right) - \frac{1}{2}\tan^{-1}\left(\frac{1}{H}\right) + \frac{1}{4\sqrt{2}}\ln\left(\frac{1 + \sqrt{2H + H^2}}{1 - \sqrt{2H + H^2}}\right) - \frac{1}{2\sqrt{2}}\tan^{-1}\left(\frac{\sqrt{2H}}{H^2 - 1}\right) \tag{11}$$

[2] Here the sign convention for $G_1(H)$ is the opposite of that used in Paper I.

The feedback effect always opposes the drift because a density maximum (minimum) of the disturbance always leads (trails) the drifting protoplanet.

The primary driver of protoplanet migration is assumed to be differential torques arising from global asymmetries in the properties of the disk as first suggested by Goldreich and Tremaine (1980). For the simple torque model used in equation (4), this requires a variation in the unperturbed density, $\sigma_0(x)$. If $\sigma_0(x)$ varies with $x$, so does the unperturbed flux seen from the moving frame. This introduces a time dependence to the unperturbed density in this frame, $\partial\sigma_0/\partial t = v_p\partial\sigma_0/\partial x$. If this is used to estimate $\partial\sigma/\partial t$, equation (6) can be integrated and equations (7) and (8) recovered with the exception that $\sigma_0(x)$ replaces $\sigma_0$. This is equivalent to again assuming the flux is unchanged from its unperturbed value, which is not strictly correct. An improvement to equation (8) can be found by using its time derivative in equation (6) and again integrating. This iterative procedure yields a correction of order $\sigma'/\sigma \sim O(h/r)^2$ which can be ignored to the level of accuracy sought here.

*c) Drift Rates*

Keeping linear terms in a Taylor expansion of $\sigma_0$; $\sigma_0(x) = \sigma_0(1 - kx/r)$, where $k = -(r/\sigma_0)\partial\sigma_0(r)/\partial r$ is a constant of order unity parameterizing the density gradient. Substituting $\sigma_0(x)/(1 - v/v_p)$ into equation (4) gives

$$v_p = 2\mu f\frac{\sigma_0 r^2}{M_\odot}\left(\frac{r}{h}\right)^2 (r\Omega)\left[kH^2 G_2(H) - \left(\frac{r}{h}\right)H^3 G_1(H)\right] \tag{12}$$

where

$$G_2(H) = \frac{H^6}{H^8 - 1} + \frac{1}{4}\ln\left(\frac{H^2 + 1}{H^2 - 1}\right) + \frac{1}{2}\tan^{-1}\left(\frac{1}{H^2}\right) . \tag{13}$$

Equation (9) can be used to eliminate $H$, yielding a single relationship between $v_p$ and $\mu$. In practice, it is easier to eliminate $v_p$ and obtain $\mu(H)$,

$$\mu = 2\left[k\frac{G_2(H)}{H^2} - \left(\frac{r}{h}\right)\frac{G_1(H)}{H}\right]\left(\frac{\pi\sigma_0 h^2}{M_\odot}\right) = \mu^*(H, h, k)\left(\frac{\pi\sigma_0 h^2}{M_\odot}\right) \tag{14}$$

and use equation (14) with either equation (9) or (12) to find its associated drift rate. The behavior of $\mu(H)$ is shown in Figure 1 for several values of $k$ and $h$. The inverse function $H(\mu)$ is clearly double valued, and thus so is $v_p(\mu)$. More importantly, there is a critical value, $\mu_{\max}{}^*$, above which solutions do not exist. This sets the inertial limit, $\mu_i = \mu_{\max}{}^*(\pi\sigma_0 h^2/M_\odot)$. Objects of greater mass cannot sustain steady drift and will stall, opening a gap in the disk. For nominal values used in Paper I, $k = 3/2$, $h/r = 0.1$; $\mu_{\max}{}^* \sim 0.2$. In general it is a function of $h$ and $k$—not a constant, as inferred in LP86.

The nature of $\mu_{\max}{}^*(h, k)$ is easy to display. We first expand $G_1(H)$ and $G_2(H)$ as power series in $1/H$ (see Appendix). Although the last four terms in $G_1$ contain contributions of order $1/H^n$ for all odd $n$, these mutually cancel through fifth order, leaving $G_1(H) = 16/7(1/H)^7 + O(1/H)^{15} + \ldots$. The second function can be expanded as $G_2(H) = 2(1/H)^2 + O(1/H)^{10} + \ldots$. Hence to lowest order $\mu^*$ takes the form

$$\mu^*(H, k, h) \sim \frac{4}{H^4}\left[k - \frac{8}{7}\left(\frac{r}{h}\right)\frac{1}{H^4}\right] . \tag{15}$$

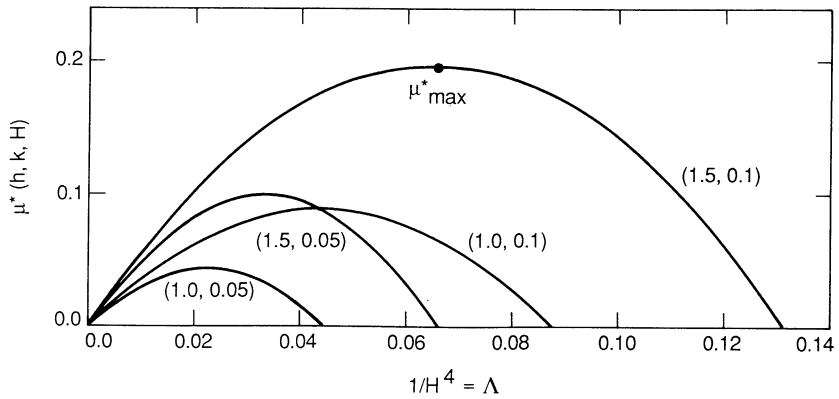


FIG. 1.—Perturber mass normalized to $\pi\sigma h^2$ as a function of the disturbance parameter $\Lambda = 1/H^4$ and $(k, h/r)$

This approximation is quite good for positive (physically meaningful) $\mu^*$ and has a maximum at $\Lambda_c = 1/H_c^4 = (7/16)\ kh/r$ with a value $\mu_{max}{}^* = (7/8)k^2h/r$. (Note $\mu_{max}{}^* = 0.197$ for $k = 3/2$, $h/r = 0.1$, in excellent agreement with Paper I.) The inertial mass limit can thus be written

$$\mu_i = \mu_{max}{}^*(h, k)\left(\frac{\pi\sigma_0 h^2}{M_\odot}\right) \approx \frac{7}{8}k^2\left(\frac{h}{r}\right)\left(\frac{\pi\sigma_0 h^2}{M_\odot}\right) \qquad (16)$$

For $\mu < \mu_i$, the drift velocity can be found from equation (9) with the aid of equations (15) and (16),

$$v_p = 2kf\mu_i\left(\frac{r}{h}\right)^2\left(\frac{\sigma_0 r^2}{M_\odot}\right)(r\Omega)\left[\frac{(\mu/\mu_i)^2}{1 \pm (1 - \mu/\mu_i)^{1/2}}\right]. \qquad (17)$$

The combination of terms preceding the last bracket gives the drift speed $v_i$ for an object equal to the inertial mass. Equation (17) is shown in Figure 2. There are two branches; an upper, stable one and lower, unstable one. Interestingly, $\mu_i$ is not the fastest migrating mass; $v_{max} \cong 1.19v_i$ occurs for $\mu/\mu_i = \frac{8}{9}$. For $\mu \ll \mu_i$, the stable branch is

$$v_0 \approx 2v_i\left(\frac{\mu}{\mu_i}\right) = 4kf\mu\left(\frac{r}{h}\right)^2\left(\frac{\sigma_0 r^2}{M_\odot}\right)(r\Omega)\ . \qquad (18)$$

Equation (18) would also be the velocity obtained in the *absence* of a tidal feedback from the disk.

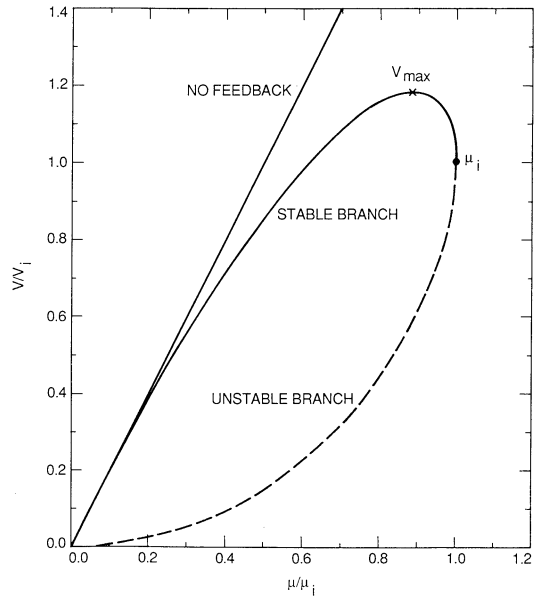


FIG. 2.—Drift velocity as a function of perturber mass. Upper branch is stable, lower branch is unstable. Both branches terminate at the inertial limit. The drift velocity in the absence of tidal disturbance of the disk is also shown.

## III. NUMERICAL MODELS

To compare our results with those of Lin and Papaloizou we first bring our torque model into coincidence with theirs by adopting their form of the cutoff function. This changes the lead terms of $G_1(H)$ and $G_2(H)$ to $H^5 \ln[(H^4 + 1)/(H^4 - 1)] - 2H$ and $H^{10} \ln[(H^4 + 1)/(H^4 - 1)] - 2H^6$, respectively. Both the direct driving and feedback components of equation (12) are weakened, but the latter more so. This turns out to raise the inertial limit slightly to $\mu_i \sim (35/24)k^2(h/r)\pi\sigma_0 h^2/M_\odot$. The drift velocity can again be found from equation (17) after replacing the lead coefficient of 2 with 5/3.

Lin and Papaloizou parameterize their case studies through the combination $B \equiv 3\pi\Sigma_0 R_0{}^2/m$, where $(R_0, \Sigma_0)$ are reference values related to local values of $(r, \sigma_0)$ by $r/R_0 = r' = 0.701$ and $\sigma_0/\Sigma_0 = 1 - r'$ for the models in question. Our critical mass is derived in terms of local values. The logarithmic derivative $k = -(r/\sigma)d\sigma/dr = r'(\Sigma_0/\sigma_0) = r'/(1 - r') = 2.34$ and $m_i$ can be written $1.46(r'/1 - r')(h/R_0)\pi\Sigma_0 h^2$ in terms of their reference values. Our theory then predicts a critical value $B_{crit} = 2.05(1 - r')r'^{-1}(R_0/h)^3 = 0.876(R_0/h)^3$ above which gap formation should be inhibited. Since their model also tracks the possible viscous evolution of the disk, they introduce a second parameter $A \equiv R_0{}^2\Omega_0\mu^2 f/(3\pi\nu_0)$, which is a measure of the relative strength of tidal to viscous effects. Viscous diffusion can inhibit gap development by a stationary protoplanet when $A \ll A_{crit} \sim (h/R_0)^3$, (LP86, after correcting a typographical error in that paper).

Table 1 lists their case studies. Since they varied $h/R_0$ as well as $A$ and $B$, it is more revealing to compare $A/A_{crit}$ and $(B/B_{crit})^{-1} = \mu/\mu_i$, *both* of which should exceed unity for a gap to form. These ratios are also listed in Table 1 and a map of their distribution in parameter space is provided in Figure 3. Although the outcomes of their experiments appear to agree with expectations, it is clear that insufficient parameter space was explored to test for the inertial limit. Case II, which they claimed to be a decisive test is, in fact, almost on the boundary

TABLE 1

SUMMARY OF LP 86 MODEL PARAMETERS

| Model | $A$ | $B$ | $h/r$ | $A_{crit}$ | $B_{crit}$ | $A/A_{crit}$ | $B_{crit}/B$ | Gap? |
|---|---|---|---|---|---|---|---|---|
| I ..... | $10^{-5}$ | $10^5$ | 0.01 | $10^{-6}$ | $8.8 \times 10^5$ | 10.0 | 8.8 | yes |
| II ..... | $10^{-5}$ | $10^6$ | 0.01 | $10^{-6}$ | $8.8 \times 10^5$ | 10.0 | 0.88 | yes |
| III ..... | $10^{-6}$ | $10^5$ | 0.01 | $10^{-6}$ | $8.8 \times 10^5$ | 1.0 | 8.8 | yes |
| IIIa ..... | $10^{-6}$ | $10^5$ | 0.02 | $8 \times 10^{-5}$ | $1.1 \times 10^5$ | 0.125 | 1.1 | no |
| IV ..... | $10^{-5}$ | $10^5$ | 0.02 | $8 \times 10^{-5}$ | $1.1 \times 10^5$ | 1.25 | 1.1 | yes |
| IVa ..... | $10^{-5}$ | $10^6$ | 0.02 | $8 \times 10^{-5}$ | $1.1 \times 10^5$ | 1.25 | 0.11 | no |

of the region of gap formation. This confusion stems from their uncritical use of $\mu_{max}^* = 0.2$, a value appropriate for our model disk in Paper I but not for theirs. The proper value for case II is $\mu_{max}^* = 0.114$ (see below). Gap formation was inhibited in two cases; III*a* which is well within the regime where diffusion should overpower the tidal forces, and case IV*a* where the mass of the perturber does lie below the inertial limit, but diffusion, although marginal, may still contribute. Significantly, case IV—with the same value of $A/A_{crit}$ as IV*a*, but a mass above the inertial limit— exhibits gap formation, implying that it is, indeed, this trait that accounts for their dissimilar outcomes. Unfortunately, less equivocal examples were not provided by Lin and Papaloizou. We remedy that deficiency below.

To isolate the feature of interest, the disk is assumed to be inviscid for which $A \to \infty$. Thus only the migration of the protoplanet can prevent the formation of a gap. In a fixed coordinate frame, the continuity equation reads

$$\frac{\partial \sigma}{\partial t} \approx -\frac{\partial}{\partial x}(\sigma v) = -\frac{f\mu^2\Omega r^5}{\pi}\frac{\partial}{\partial x}\left[\frac{\sigma f(x - x_p)}{(x - x_p)^4}\,\mathrm{sgn}\,(x - x_p)\right], \tag{19}$$

where $\sigma = \sigma(x, t)$ is time dependent, $x$ measures positions in the disk and $x_p(t)$ the location of the perturber—both taken with respect to the perturber's initial position. Slowly changing variables are again treated as constant. Equation (19) can be cast into a convenient nondimensional form by normalizing distances to the scale height, surface densities to the value at the starting position of the perturber, $\sigma_{0,0} = \sigma(0, 0)$, and the time variable to the interval needed for a stationary object to clear a gap of width $h$; $\tau_{gap} = (\pi/f\mu^2\Omega)(h/r)^5$ (see Paper I). This procedure yields,

$$\frac{\partial \sigma'}{\partial t'} \approx -\frac{\partial}{\partial x'}\left[\frac{\sigma' f(x' - x_p')}{(x' - x_p')^4}\,\mathrm{sgn}\,(x' - x_p')\right], \tag{20}$$

where primes denote normalized quantities. Similarly, equation (4) can be written in the nondimensional form,

$$v_p' = \frac{dx_p'}{dt'} = -\frac{2}{\mu^*}\left(\frac{r}{h}\right)\int \frac{\sigma' f(x' - x_p')}{(x' - x_p')^4}\,\mathrm{sgn}\,(x' - x_p')dx', \tag{21}$$

where $\mu^* = m/\pi\sigma_{0,0}h^2$. In order to facilitate comparison with LP86, the linear form of the cut-off function is used: i.e., $f(x' - x_p') = |x' - x_p'|^5$ for $|x' - x_p'| < 1$, otherwise unity. The initial density profile is $\sigma' = 1 - k(h/r)x'$ where $h/r$ is the ratio of the scale height to the heliocentric position of the perturber. Since $r = r'R_0$ in LP86, their choice of $h/R_0 = 0.01$ and $r' = 0.701$ is equivalent to setting $h/r = (h/R_\odot)/r' = 0.0143$. This, together with $k = r'/(1 - r') = 2.34$ establishes the critical value $\mu_{max}^* = 0.114$ mentioned above.

Equations (20) and (21) were integrated by a finite difference scheme for several values of $k$, $h/r$, and $\mu^*$. Table 2 indicates whether a gap develops in each case. The results are in excellent agreement with theoretical predictions. Because of the starting density profile, all cases exhibit a transitory migration phase during which the disk adjusts to the tidal torque. (It is not at all obvious that this is a reasonable starting condition. The perturber is not "turned on" suddenly, but acquires its mass through accretion and therefore has a history of interaction with the disk. Again, our use of a linear profile is to

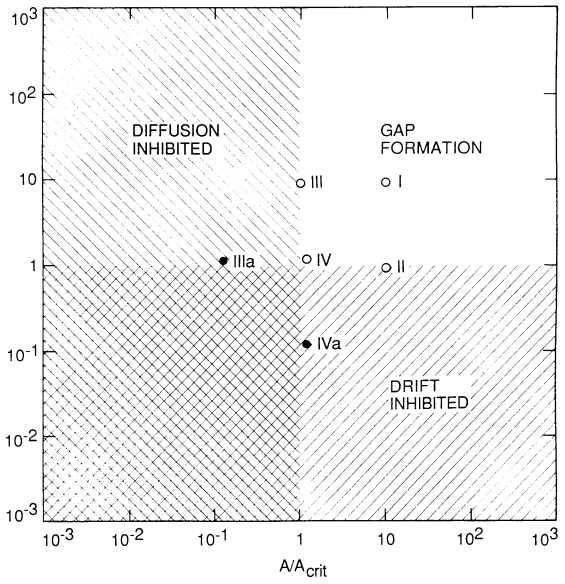


FIG. 3.—Distribution of case studies in LP86 compared to gap criteria. Open circles indicate development of a gap in the disk; closed circles denote cases where gap is inhibited.

TABLE 2

GAP FORMATION

| $k$ | $h/r$ | $\mu_{max}^*$ | $\mu^*$ | $\mu^*/\mu_{max}^*$ | Gap? |
|---|---|---|---|---|---|
| 2.34..... | 0.0143 | 0.114 | 0.091 | 0.80 | no |
| | | | 0.103 | 0.90 | no |
| | | | 0.114 | 1.00 | no |
| | | | 0.125 | 1.10 | yes |
| | | | 0.137 | 1.20 | yes |
| 2.34..... | 0.0285 | 0.228 | 0.228 | 1.00 | no |
| | | | 0.251 | 1.10 | yes |
| 1.00..... | 0.05 | 0.0729 | 0.060 | 0.82 | no |
| | | | 0.070 | 0.96 | no |
| | | | 0.080 | 1.10 | yes |
| | | | 0.090 | 1.23 | yes |

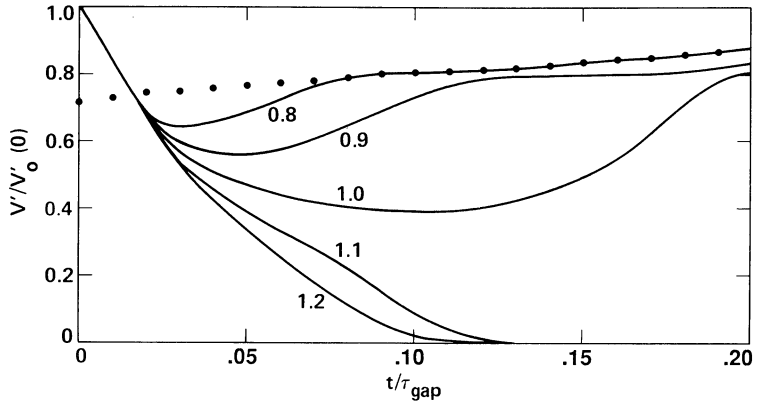


FIG. 4.—Velocity as a function of time found by numerical integration for $(k, h/r) = (2.34, 0.0143)$ models. Curves are labeled by values of $\mu^*/\mu_{max}^*$ where $\mu_{max}^* = 0.114$. Dotted line indicates quasi-steady state velocity curve for $\mu^*/\mu_{max}^* = 0.8$. Velocities have been normalized to zero feedback values.

facilitate comparison with LP86.) The initial drift velocity can be found from integrating equation (21) at $t' = 0$,

$$v_0'(t' = 0) = \frac{10}{3}\frac{k}{\mu^*} \tag{22}$$

and simply represents the velocity in the absence of tidal feedback (eq. [18]) for the linear cutoff model. As the evolution proceeds, the velocity quickly decays from this starting value. Objects large enough to open a gap eventually become trapped, with their velocities decaying toward zero. Objects escaping this fate should have velocity curves that approach the quasi-steady state curve predicted in equation (17),

$$v' = \frac{1}{2} v_0' \left[\frac{\mu/\mu_i}{1 - (1 - \mu/\mu_i)^{1/2}}\right]. \tag{23}$$

Figure 4 shows the velocity curves for the models most closely resembling those of Lin and Papaloizou, i.e., the first entries in Table 2. With these models, the effective logarithmic derivative $k \propto \sigma^{-1}$ and $\mu_i \propto k^2\sigma \propto \sigma^{-1}$. Hence, the inertial mass rises slightly as the perturber migrates outward; $\mu_i(x') \rightarrow \mu_i(0)/[1 - k(h/r)x']$. This causes a slow increase in $v'/v_0'$ from equation (23). The steady state velocity curve for $\mu^* = 0.80$ is shown in Figure 4 as an example. After a transitory adjustment period, the velocity approaches the steady state curve and follows it closely. This was a general feature of all cases considered where gap formation did not occur. Interestingly, we *did not* find gap formation for $\mu^*/\mu_{max}^* = 0.9$, in contrast to the results reported in LP86 (case II, equivalent to $\mu^*/\mu_{max}^* = 0.88$). We cannot explain this discrepancy, but do find the close agreement between our analytic and numerical work reassuring. Figure 5 compares the surface density of the disk at $t = 0.1\tau_{gap}$ for masses below, at, and above the critical. The "smoothing" of the global gradient at the critical mass is clearly illustrated, while, for the slightly larger mass, gap development is well underway.

## IV. DISCUSSION

It is mostly the interpretation, not the calculations, in LP86 with which we take exception. Indeed, their results are generally consistent with our model's predictions when the scaling factor $\mu^*(h, k)$ is properly determined for their study conditions. Their assertion that we adopted a fixed surface density profile that "... inadequately describes the disk response to the protoplanet's tides" is based on an unfortunate misinterpretation of our procedure. We, perhaps, bear some responsibility for this, since our introductory remarks motivating the calculations in Paper I (and similar to those made in the introduction to this paper), compared planetesimal drift times to the time to clear a gap, which is typically $\mathcal{O}(r/h)$ longer than required to smooth out a weak density gradient. This distinction was stressed in LP86, and we concur. Indeed, our calculations *do* correctly use the tidal disturbance of the disk to evaluate its feedback effect. Qualitatively, this effect is to induce a local density gradient that opposes and partially compensates for the global one. The degree of compensation

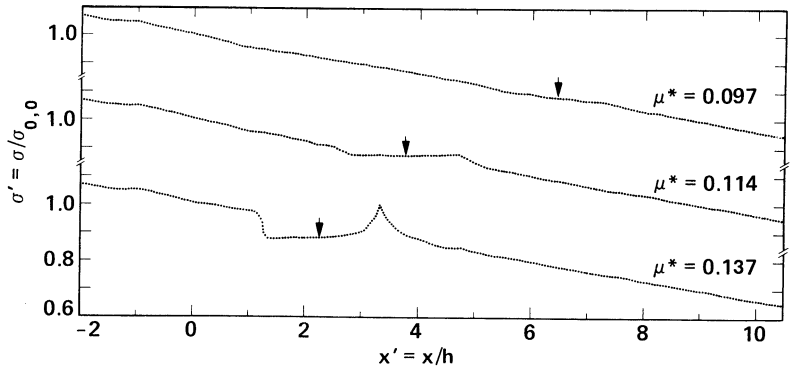


FIG. 5.—Surface density profiles at $t' = t/\tau_{gap} = 0.1$ for $(k, h/r) = (2.34, 0.0143)$ models. Arrow indicates position of perturber; distance is measured in scale heights. Top curve shows sustained migration without gap development for a mass less than the inertial limit. Middle curve displays nearly complete compensation of the global gradient at the limiting mass ($\mu_{max}^* = 0.114$). For a slightly larger object (*bottom curve*) migration stalls and a gap quickly opens.

increases with mass, becoming essentially complete at the inertial limit (Fig. 5). Again, this is quite consistent with the behavior reported in LP86 and with that found in our own numerical work. Accordingly, *we find no basis for their conclusion that "... there is not an inertial limit as proposed by Hourigan and Ward (1984)."*

Although it is relatively easy to establish the theoretical existence of an inertial limit, it is, of course, more problematical whether it actually operated in the early solar system. For migration to dominate viscous effects, $\mu_i$ must exceed $\mu_\nu$, a second critical mass associated with viscous diffusion (Paper I). This sets a limit on the viscosity of, $\nu/(c^2\Omega^{-1}) = \alpha \lesssim (h/r)(\sigma r^2/M_\odot)^2 \sim \mathcal{O}(10^{-9} - 10^{-7})$. This is considerably less than turbulent viscosity estimate of $\alpha \sim \mathcal{O}(10^{-4})$ for iron grain opacities made recently by Cabot *et al.* (1987). However, this value is predicated on the presence of abundant fine-grained material to provide the requisite opacity. In the later stages of planetary accretion, it remains unclear whether there will be sufficient opacity to sustain turbulent convection (e.g., Weidenschilling 1984).

Finally we should point out that the torque model represented by equation (1) is a considerable oversimplification. Since our main objective has been to reconcile the numerical experiments of Lin and Papaloizou with our own earlier analysis, we have employed the same torque model originally used in both studies. More recent work (Ward 1986) indicates that in a Keplerian disk, a differential torque can arise from asymmetries in resonance locations alone. This net torque is negative, resulting in orbital decay, because outer Lindblad resonances lie slightly closer to the perturber. In addition, a pressure gradient due to density or temperature gradients can also influence torque estimates by shifting resonance positions. Finally, an important assumption underlying both our work and that of Lin and Papaloizou is that density waves damp locally. If, in fact, density waves propagate out of the local zone ($\gg h$), gap formation will be further inhibited and the inertial limit larger (Ward, 1986). These features should eventually be incorporated into an improved model of protoplanet migration, but we defer such a task to a later publication.

Unfortunately, we missed the 1986 paper by Lin and Papaloizou when it was published, and remained unaware of their paper until late 1987, when a colleague brought it to our attention. For this, we wish to express our appreciation to C. F. Yoder. W. R. W. wishes to also thank the Department of Physics, Harvey Mudd College, for their hospitality during a portion of this research project. This research was supported by NASA under NBAS-100 with the Jet Propulsion Laboratory, California Institute of Technology.

## APPENDIX

The expansion of the function $G_1(H)$ is as follows:

$$\frac{2H}{H^8 - 1} = 2\left[\left(\frac{1}{H}\right)^7 + \left(\frac{1}{H}\right)^{15} + \cdots\right], \tag{A1}$$

$$\frac{1}{4}\ln\left(\frac{H+1}{H-1}\right) = \frac{1}{2}\left[\left(\frac{1}{H}\right) + \frac{1}{3}\left(\frac{1}{H}\right)^3 + \frac{1}{5}\left(\frac{1}{H}\right)^5 + \frac{1}{7}\left(\frac{1}{H}\right)^7 + \cdots\right], \tag{A2}$$

$$\frac{1}{2}\tan^{-1}\left(\frac{1}{H}\right) = \frac{1}{2}\left[\left(\frac{1}{H}\right) - \frac{1}{3}\left(\frac{1}{H}\right)^3 + \frac{1}{5}\left(\frac{1}{H}\right)^5 - \frac{1}{7}\left(\frac{1}{H}\right)^7 + \cdots\right], \tag{A3}$$

$$\frac{1}{4\sqrt{2}}\ln\left(\frac{1+\sqrt{2H+H^2}}{1-\sqrt{2H+H^2}}\right) = \frac{1}{2}\left[\left(\frac{1}{H}\right) - \frac{1}{3}\left(\frac{1}{H}\right)^3 - \frac{1}{5}\left(\frac{1}{H}\right)^5 + \frac{1}{7}\left(\frac{1}{H}\right)^7 - \cdots\right], \tag{A4}$$

$$\frac{1}{2\sqrt{2}}\tan^{-1}\left(\frac{\sqrt{2H}}{H^2-1}\right) = \frac{1}{2}\left[\left(\frac{1}{H}\right) + \frac{1}{3}\left(\frac{1}{H}\right)^3 - \frac{1}{5}\left(\frac{1}{H}\right)^5 - \frac{1}{7}\left(\frac{1}{H}\right)^7 + \cdots\right]. \tag{A5}$$

The expansion of $G_2(H)$ is

$$\frac{H^6}{H^8 - 1} = \left(\frac{1}{H}\right)^2 + \left(\frac{1}{H}\right)^{10} + \cdots, \tag{A6}$$

$$\frac{1}{4}\ln\left(\frac{H^2+1}{H^2-1}\right) = \frac{1}{2}\left[\left(\frac{1}{H}\right)^2 + \frac{1}{3}\left(\frac{1}{H}\right)^6 + \frac{1}{5}\left(\frac{1}{H}\right)^{10} + \cdots\right], \tag{A7}$$

$$\frac{1}{2}\tan^{-1}\left(\frac{1}{H^2}\right) = \frac{1}{2}\left[\left(\frac{1}{H}\right)^2 - \frac{1}{3}\left(\frac{1}{H}\right)^6 + \frac{1}{5}\left(\frac{1}{H}\right)^{10} - \cdots\right]. \tag{A8}$$

## REFERENCES

Cabot, W., Canuto, V. M., Hubickyj, O., and Pollack, J. B. 1987, *Icarus*, **69**, 423.
Goldreich, P., and Tremaine, S. 1979, *Ap. J.*, **233**, 857.
———. 1980, *Ap. J.*, **241**, 425.
Hourigan, K., and Ward, W. R. 1984, *Icarus*, **60**, 29.
Lin, D. N. C., and Papaloizou, J. 1979, *M.N.R.A.S.*, **186**, 789.
———. 1986, *Ap. J.*, **309**, 846 (LP86).
Lynden-Bell, D., and Pringle, J. E. 1974, *M.N.R.A.S.*, **168**, 603.
Ward, W. R. 1986, *Icarus*, **67**, 164.
Weidenschilling, S. J. 1984, *Icarus*, **60**, 553.

KERRY HOURIGAN: Division of Building, Construction, and Engineering, CSIRO, Highett, Victoria 3190, Australia

WILLIAM R. WARD: Geology and Planetology Section, Jet Propulsion Laboratory, California Institute of Technology, Pasadena, CA 91109